Available online at BCREC website: https://bcrec.id

Bulletin of Chemical Reaction Engineering & Catalysis, 17 (1) 2022, 216-224

Research Article

Synthesis of Mesoporous Carbon from Merbau Sawdust as a Nickel Metal Catalyst Support for Castor Oil Hydrocracking

Wega Trisunaryanti[1*], T. Triyono[1], Suryo Purwono[2], Aprilia Siti Purwanti[1], Satriyo Dibyo Sumbogo[1]

[1]Department of Chemistry, Faculty of Mathematic and Natural Science, Universitas Gadjah Mada, Yogyakarta, Indonesia
[2]Department of Chemical Engineering, Faculty of Engineering, Universitas Gadjah Mada, Yogyakarta, Indonesia

Received: 25th November 2021; Revised: 15th February 2022; Accepted: 16th February 2022
Available online: 19th February 2022; Published regularly: March 2022

Abstract

Synthesis of mesoporous carbon from merbau sawdust with H_2O_2 as activator using reflux method followed by carbonization at 800 °C (RC800) had been carried out. This research is aiming to produce effective pathway to synthesize effective nickel-mesoporous carbon catalyst. The nickel metal was impregnated on the mesoporous carbon by wet impregnation using the salt precursor of $Ni(NO_3)_2{\cdot}6H_2O$. The results showed that carbon RC800 and C800 had a specific surface area of 135.18 and 182.48 m^2/g. Specific surface area of Ni/RC800 and Ni/C800 catalyst were 41.31 and 7.15 m^2/g, respectively. The metal content in Ni/RC800 and Ni/C800 catalyst were 0.83 and 0.92 wt%, respectively. Ni/RC800 catalyst had the highest acidity (7.64 mmol/g) compared to Ni/C800 catalyst (6.99 mmol/g), RC800 (97.43 mmol/g), and C800 (6.17 mmol/g). The Ni/RC800 catalyst has the highest activity with the liquid product conversion of 66.01 wt%. Its selectivity towards gasoline fraction, diesel fraction, alcohol, and organic was 8.06, 1.17, 2.61, and 54.13%, respectively.

Keywords: hydrocracking; mesoporous carbon; castor oil; sawdust; nickel

How to Cite: W. Trisunaryanti, T. Triyono, S. Purwono, A.S. Purwanti, S.D. Sumbogo. (2022). Synthesis of Mesoporous Carbon from Merbau Sawdust as a Nickel Metal Catalyst Support for Castor Oil Hydrocracking. *Bulletin of Chemical Reaction Engineering & Catalysis*, 17(1), 216-224 (doi: 10.9767/bcrec.17.1.12940.216-224)

Permalink/DOI: https://doi.org/10.9767/bcrec.17.1.12940.216-224

1. Introduction

The search for alternate hydrocarbon fuel source has been major global challenge. According to British Petroleum, the global oil consumption rose from 3.93 billion tonnes to 4.33 billion tonnes in 2005-2015 period, it could be predicted that the rising trend would likely to happened. [1] Vegetable oils posed great potential for commercial use as these sources contains relatively high content of triglycerides that can be converted into hydrocarbon fuel [2-3]. However, edible vegetable oils cannot be cultivated into fuels as they compete with food demand [2-4]. Therefore, non-edible vegetable oil such as Castor oil (*Ricinus communis L.*) could be used as alternate source, as this oil is not suitable for consumption because it contains ricin and ricinin (two highly toxic proteins). [5-10]. Castor oil also contains 80-90% ricinoleic acid that can be converted into hydrocarbon [9].

* Corresponding Author.
Email: wegats@ugm.ac.id (W. Trisunaryanti)

Converting castor oil into hydrocarbon can be done through hydrocracking process. [8-10].

Hydrocracking uses heterogenous catalyst to provide efficient path for vegetable oils conversion into fuel [10-12]. Mesoporous catalyst support has been widely used in heterogenous catalyst system, such as silica-alumina [8,13], silica [14,15], and activated carbon [3, 16]. Among all the candidates, activated carbon promised great potential as this material is cheap, has thermal stability, and have functional groups that can bind with metal and feed in hydrocracking process.

Activated carbon could be produced from cheap materials such as wood sawdust from wood cutting factory as they contain lignin and cellulose [17-19]. Not only activated carbon could be produced from cheap source, but they also have wide versatility towards pore modification. Hydrocracking process demands catalyst that has low limitation of feed mass transfer into its active sites. The size of lipid molecule that is normally larger than 2 nm is too large for micropore, hence, the diameter of the catalyst should be at least in mesoporous range [20]. The synthesis of mesoporous carbon can be done in the activation process of the material [21-23]. Hydrogen peroxide was known in previous study that it can gives large number of functional groups and produced highly porous carbon, compared to KOH and H_3PO_4 [24]. The activation of carbon can be done using H_2O_2 under reflux conditions, where H_2O_2 can create oxygenated functional groups while creating more pores of activated carbon [24]. The H_2O_2 as an oxidizing agent can oxidize carbon deposits that cover pores and thus when heated, it can open more pores of activated carbon. Although activated carbon has functional groups that can act as catalytic acid site, metal impregnation is still needed as metal could increase the catalyst acidity, hence could gives better performance in hydrocracking [25]. Nickel was known in our previous study that it has good selectivity towards gasoline fraction products [26]. No research has yet confirmed that activated carbon from H_2O_2 activation and its impregnated state is suitable for hydrocracking application of vegetable oil, such as castor oil.

In this research, homogeneous and heterogeneous catalysts were used for the hydrocracking process. Homogeneous catalyst in the form of mesoporous carbon which synthesized from merbau sawdust with carbonization at 800 °C (C800) and mesoporous carbon activated with H_2O_2 using reflux method followed by carbonization at 800 °C (RC800). Heterogeneous catalysts were in the form of C800 and RC800 catalyst with 1% Ni metal, which further were called Ni/C800 and Ni/RC800. The catalyst hydrocracking performance was tested towards castor oil.

2. Materials and Methods

2.1 Materials

Merbau sawdust was collected from Manokwari Regency, West Papua, Indonesia. Castor oil was purchased from local store. $Ni(NO_3)_2{\cdot}6H_2O$ and H_2O_2 were purchased from Merck. The gases used in this research (N_2 and H_2) were supplied by PT Surya Indotim Imex.

2.2 Characterization Instruments

The functional groups of all samples were elucidated using Fourier Transform Infra-Red Spectroscopy (FTIR, Shimadzu Prestige-21) equipped with data station in the range of 4000–400 cm^{-1} with a KBr disc technique. The surface parameters (surface area, pore diameter, and total pore volume) of all samples were measured using Gas Sorption Analyzer (GSA, NOV-1200e Quantachrome), the surface areas were calculated by the Brunaeur-Emmett-Teller (BET) method, and the pore size distributions were calculated by the Barret-Joyner-Halenda (BJH) method. The surface morphology of the catalysts and their nickel content were taken using a Scanning Electron Microscope (SEM-EDX, JEOL JSM-6510LA). The X-Ray Diffraction (XRD, X'Pert PRO PAN analytical) was used to observe the crystallinity of the catalysts. The liquid products of hydrocracking process were analyzed using Gas Chromatography-Mass Spectrometry (GC-MS, Shimadzu QP2010S).

2.3 Procedures

2.3.1 Synthesis and characterization of mesoporous carbon C800 and RC800

The synthesis of activated carbon, named C800, was carried without reflux. The dried merbau sawdust was immediately carbonized at 800 °C for 2 h under nitrogen gas flow of 20 mL/min. Mesoporous carbon synthesized from merbau sawdust by carbonization at 800°C.

The synthesis of mesoporous carbon, named RC800, was carried out through reflux using H_2O_2 as chemical activator. First, the sawdust of merbau wood (250 g) was dried using oven at 105 °C for 3 h. Then, 15 g of the dried wood was refluxed with 90 mL H_2O_2 at 100 °C for 1 h. The product then filtered and washed thoroughly with deionized water until the pH is

neutral, and then dried again at 105 °C for 24 hours. The dried product were carbonized at 800 °C for 2 h under nitrogen gas flow of 20 mL/min.

2.3.2 Preparation of Metal Impregnated Carbon Catalyst

The carbon synthesized from previous methods, C800 and RC800, were used as support material for nickel impregnation. Exactly, 0.0495 g of $Ni(NO_3)_2{\cdot}6H_2O$ salt was dissolved in 30 mL deionized water. The solution was added with 1 g of carbon that had been sieved 80 mesh and subsequently stirred with a magnetic stirrer at 80 °C for 2 hours, and then dried at 105 ° C for 7 hours. The dried catalyst was calcined at 400 °C for 3 hours under nitrogen gas flow of 20 mL/min and reduced at 400 °C for 3 hours under hydrogen gas flow of 20 mL/minute.

2.3.4 Acidity test of carbon and catalyst

The acidity test was determined quantitatively using gravimetric method. This method compares the weight of catalyst before and after adsorption of ammonia gas (NH_3), in which the measurements is based on the amount of ammonia gas absorbed by the catalyst, which assumed to be relatively equivalent to the number of catalyst acid sites. The acidity of the catalyst can be calculated by Equation (1).

$$Acidity = \frac{w_3 - w_2}{(w_2 - w_1).MW_{ammonia}} x\ 1000\ mmol/g \quad (1)$$

where, w_1 is weight of empty porcelain crucible (g), w_2 is weight of porcelain crucible contain dried catalyst (g), w_3 denotes weight of porcelain crucible and sample after adsorption (g), and $MW_{ammonia}$ is equal to 17.0303 g/mol.

2.3.5 Castor oil hydrocracking

Hydrocracking process was carried out by placing 0.1 g of catalyst and 3 g of liquid feed (castor oil) in a stainless steel semi-batch reactor at 400 °C under hydrogen gas flow of 30 mL/min for 2 h. The liquid fraction product were weighed and then analyzed using GC-MS instrument to determine the catalyst selectivity towards short range of hydrocarbon products. Yield of reaction products were calculated as:

$$Yield\ of\ Residue = \frac{w_U}{w_F} x100\% \quad (2)$$

$$Yield\ of\ Liquid\ fraction = \frac{w_P}{w_F} x100\% \quad (3)$$

$$Yield\ of\ Coke = \frac{w_{C2} - w_{C1}}{w_F} x100\% \quad (4)$$

$$Yield\ of\ Gas = 100\% - Yield\ of\ (Liquid\ Fraction + Coke + Residue) \quad (5)$$

$$Yield\ of\ Gasoline = (\%\ Area\ of\ C_5\ to\ C_{12}) \times Yield\ of\ Liquid\ Fraction \quad (6)$$

$$Yield\ of\ Diesel\ Oil = (\%\ Area\ of\ C_{13}\ to\ C_{20}) \times Yield\ of\ Liquid\ Fraction \quad (7)$$

$$Yield\ of\ Alcohol = (\%\ Area\ of\ Alcohol) \times Yield\ of\ Liquid\ Fraction \quad (8)$$

$$Yield\ of\ Organic = (\%\ Area\ of\ C_xH_yO_z) \times Yield\ of\ Liquid\ Fraction \quad (9)$$

where, w_U is weight of unconverted the feed, w_F is weight of the feed, w_{C1} is weight of the catalyst before hydrotreatment, and w_{C2} denotes weight of the catalyst after hydrotreatment.

3. Results and Discussion

3.1 Synthesis and Characterization of Mesoporous Carbon

The characterization results of merbau sawdust, C800, and RC800 using FT-IR are presented in Figure 1. The absorption peaks of merbau sawdust at wavenumber 3402 cm^{-1} showed the existence of O−H stretching vibration from the hydroxyl group, the peak of 2924 cm^{-1} showed the presence of C−H stretching vibration from the alkane, the peak of 1620 cm^{-1} showed the existence of stretching vibration of C=C double bond alkene. Whereas, the absorption peaks of C800 and RC800 also showed O−H stretching vibrations from the hydroxyl

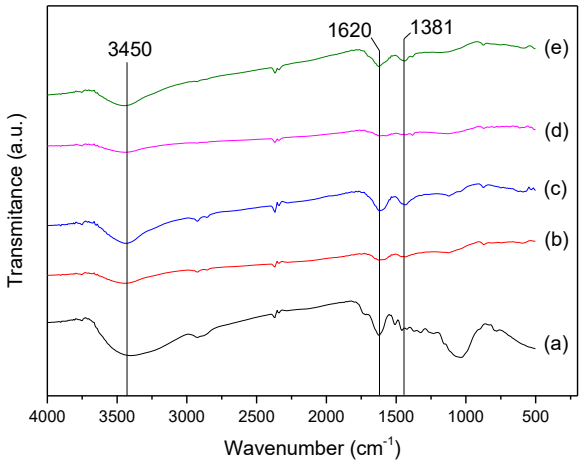

Figure 1. IR spectra of (a) merbau sawdust, (b) C800, (c) RC800, (d) Ni/C800, (e) Ni/RC800

group at wavenumbers 3448 and 3425 cm^{-1}, stretching vibrations of C=C aromatic at peaks of 1620 cm^{-1}. The peaks of 1319 cm^{-1} on the C800 and RC800 showed the presence of stretching vibrations of C–O. The presence of C=C aromatic and some functional groups, as -OH and C–O, confirmed that activated carbon, C800 and RC800, has successfully synthesized.

The adsorption isotherm of merbau sawdust is showed in Figure 2. The pattern was follow type III isotherm, which showed that the merbau sawdust was material with relatively weak adsorption strength. The adsorption isotherm graphs of C800 and RC800 are also presented in Figure 2. The patterns followed type IV adsorption isotherm. It showed that C800 and RC800 carbon were mesoporous materials.

The results of GSA analysis from merbau sawdust, C800 and RC800 showed in Table 1. The specific surface area of C800 and RC800 were much higher than merbau sawdust. It showed that pore formation in C800 and RC800 was successfully formed. It was notable that the specific surface area and average pore diameter of the C800 were higher than RC800. It was presumably due to the surface of RC800 being partially broken as a consequence of H_2O_2 effect as an activator. Although hydrogen peroxide was previously known to activate charcoal and create pores, the concentration that was used in this research was 4 times more than the previous study, where it is suspected to be too high [24].

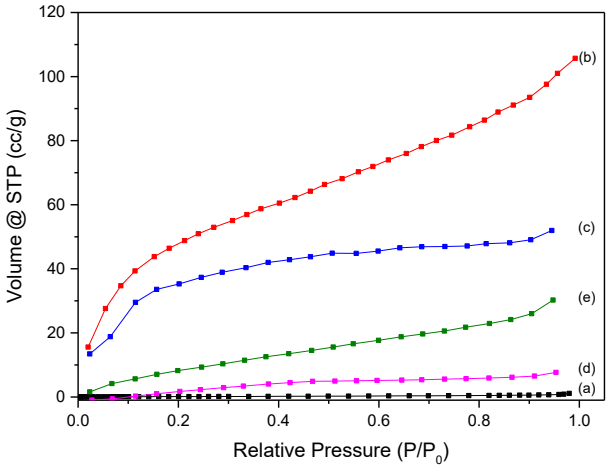

Figure 2. Isotherm adsorption graph of (a) merbau sawdust, (b) C800, (c) RC800, (d) Ni/C800, (e) Ni/RC800

Total pore volume of C800 and RC800 were much higher than merbau sawdust proved that the synthesis of C800 and RC800 was successful. Total pore volume of RC800 (1.09 cc/g) increased by 81.31% from C800 (0.60 cc/g). The usage of H_2O_2 as an activator in reflux conditions can increase the mesoporous carbon porosity due to oxidation process of carbon deposits that cover the pores. Therefore, it can open the pores of activated carbon when heated. Carbon pores thus become free from organic impurities (carbon deposits) and the properties of active sites are enhanced accordingly [25]. The combination of high number of active sites and bigger pore volumes were known to be beneficial later in the metal dispersion across the carbon matrix.

The average pore diameters of C800 and RC800 carbon were 3.58 and 2.38 nm, respectively. The values were within mesoporous range, indicated C800 and RC800 was mesoporous carbon. The pore diameter distributions of C800 and RC800 are presented in Figure 3. The dominant pore sizes of each carbon were showed by its highest peak. It can be seen in Figure 3. that activation using H_2O_2 causes trimodal distribution of pore distribution compared to C800. The pore distribution patterns of RC800 that is trimodal could indicating that the pore formation mechanism of RC800 is different to the C800.

The SEM images with 1000 times magnification of merbau sawdust, C800, and RC800 sawdust are presented in Figure 4. There were only a few pores visible in merbau sawdust because majority of the pores were closed. Whereas in C800 and RC800, the pores were seen

Table 1. Physical and chemical properties of the catalyst

Sample	Specific surface area (m^2/g)	Average pore diameter (nm)	Total pore volume (cm^3/g)	Metal Content (wt%)	Acidity (mmol/g)
Merbau sawdust	0.35	19.33	0.0017	-	-
C800	182.49	3.58	0.6	-	6.17
RC800	135.18	2.38	1.09	-	7.43
Ni/C800	7.15	3.33	0.01	0.92	6.99
Ni/RC800	41.31	2.27	0.05	0.83	7.64

with different size. C800 had larger pores than RC800, it was presumably due to the surface of RC800 being partially broken because of H_2O_2 effect.

SEM image of RC800 showed a higher number of pores than that of C800. It was due to the formation of new pores in RC800, presumably as a result of H_2O_2 usage. Higher number of pores formed during synthesis process led to the increase of the porosity of carbon, as shown in GSA analysis data that total pore volume in RC800 was higher than C800. The high porosity of mesoporous carbon will ultimately increase the catalyst activity in hydrocracking process.

The results of XRD analysis from merbau sawdust, C800, and RC800 are presented in Figure 5. Diffraction pattern from merbau sawdust was amorphous which is the property of lignin. Peaks when 2θ were 15.13 and 22.73 indicated carbon with cellulose structure. According to ICDD data 00-012-0212, the peak of C800 and RC800 appeared at 26.47 was carbon with graphite structure. Both C800 and RC800 was successfully formed, marked by the disappearance of cellulose structure and the formation of new graphitic structure.

3.2 Characterization of Ni/C800 and Ni/RC800 Catalysts

FTIR spectra of Ni/C800 catalyst was compared with spectra of C800 carbon while spectra of Ni/RC800 catalyst was compared with spectra of RC800 carbon to determine the effect of Ni metal impregnation towards the catalyst function groups as presented in Figure 1. The absorption peaks of Ni/C800 and Ni/RC800 catalysts at wave number 3448 cm^{-1} showed the presence of O−H stretching vibration from the hydroxyl group, peaks of 2862-2924 and 2931 cm^{-1} indicated the presence of C−H stretching vibrations from alkanes, peaks of 1620 cm^{-1} showed the stretching vibration of C=C alkene double bond, and peak of 1381 cm^{-1} showed the existence of a stretching vibration of C−O. Those functional groups were also found in C800 and RC800 carbon. In addition, C−O stretching vibrations of Ni/C800 and

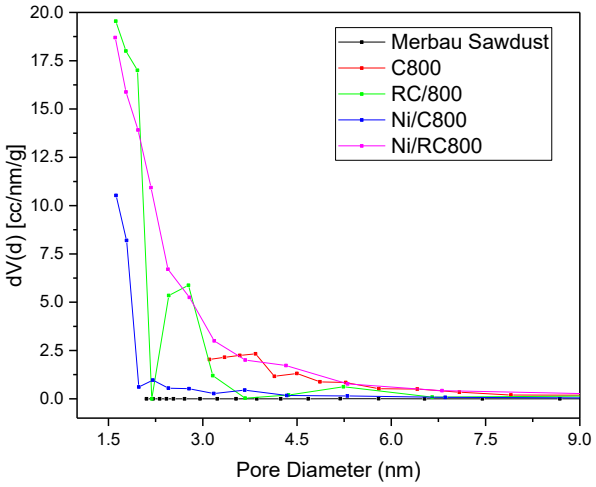

Figure 3. Pore size distribution of (a) merbau sawdust, (b) C800, (c) RC800, (d) Ni/C800, (e) Ni/RC800

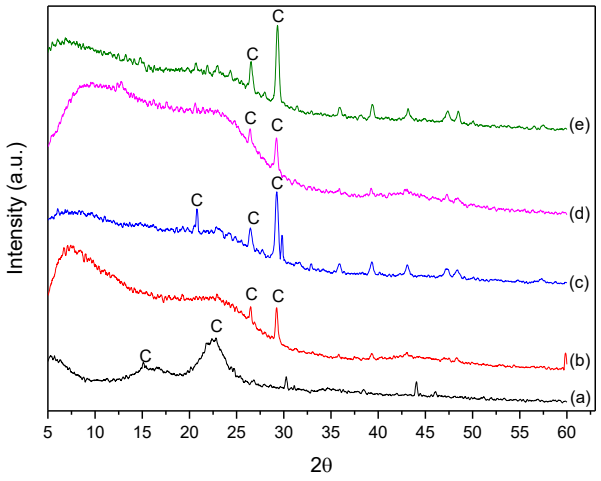

Figure 5. The diffractogram of (a) merbau sawdust, (b) C800, (c) RC800, (d) Ni/C800, (e) Ni/RC800

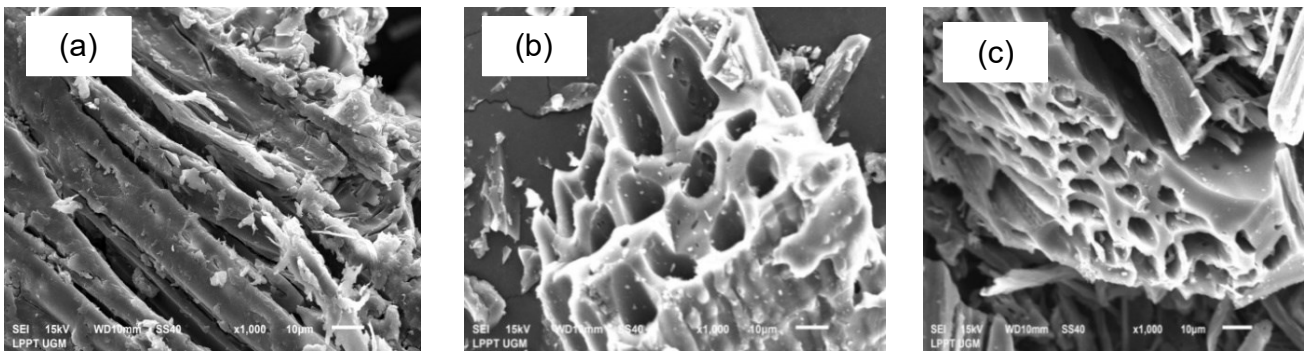

Figure 4. The SEM images of (a) merbau sawdust, (b) C800 and (c) RC800

Ni/RC800 catalysts were found at wavenumber 1381 cm^{-1}, while C−O stretching vibrations of C800 and RC800 carbon were found at wavenumber 1319 cm^{-1}. The various wavenumbers were possibly caused by the effect of Ni metal impregnated on the carbons.

The results of catalyst diffractogram is presented in Figure 5. Addition of metal peak was not found in diffractogram data, indicating that impregnated nickel metal in C800 and RC800 were distributed evenly and exist as small amorphous particles [27]. The identification of nickel metal were carried out using SEM-EDS. The percentage of Ni metal which successfully impregnated onto Ni/C800 and Ni/RC800 catalysts can be obtained from SEM-Energy Dispersive X-Ray Spectroscopy (SEM-EDS) data. The theoretical calculation of Ni metal content in each catalyst was 1 wt%. The results is presented in Table 1, where the Ni metal content in Ni/C800 catalyst was 0.92 wt%, while in Ni/RC800 was 0.83 wt%.

The results of acidity test on C800, RC800, Ni/C800, and Ni/RC800 were showed in Table 1. It shows that impregnation of Ni metal could increase the acidity of catalyst. This was due to the presence of Lewis acid sites possessed by Ni metals, thus could increase the acid sites of mesoporous carbon. The acidity level was used to determine which catalyst had better catalytic properties in hydrocracking reactions. Ni/RC800 catalyst had the highest acidity, consequently this catalyst was expected to have high catalytic activity in the hydrocracking process.

Metallic Ni impregnated onto C800 and RC800 mesoporous carbon caused the decrease of specific surface area, average pore diameter, and total pore volume of Ni/C800 and Ni/RC800 catalysts as shown in Table 1. It was due to the blocking of mesoporous carbon pores by Ni metals. The isotherm graph of Ni/C800 and Ni/RC800 catalysts followed type IV of adsorption isotherm pattern. It showed that the catalysts (Ni/C800 and Ni/RC800) were mesoporous material, as presented in Figure 2. Furthermore, the pore distribution curves of the catalysts in Figure 3 showed that both catalysts had high pore uniformity in mesoporous area. The Ni/C800 catalyst was dominated by pores with diameter of 3.24 nm while Ni/RC800 was dominated by pores with a diameter of 3.94 nm. In accordance with the SEM image results of catalyst previously, the specific surface area and total pore volume of Ni/RC800 catalyst were higher than Ni/C800 catalyst. A catalyst with high specific surface area and total pore volume has higher possibility to have good catalytic activity in the hydrocracking process.

3.3 Castor Oil Hydrocracking

The liquid products generated by the catalyst are presented in Table 2. Ni/RC800 catalyst had the highest catalytic activity. It had the highest liquid product conversion from the castor oil hydrocracking process. This could be reasoned by acidity that is highest among the four catalysts. The pores in Ni/RC800 catalyst were more open towards the feed. On the other hand, Ni/C800 has the lowest catalytic activity, even when compared to C800 or RC800. The major pore blackening in Ni/C800 could be the culprit for this phenomenon. Surface area and total pore volume of Ni/C800 catalyst were very low compared to Ni/RC800, C800, and RC800 catalyst. Although the difference of liquid product produced from each catalyst was quite slim, there is unique case where there is major improvement in liquid produced after nickel impregnation onto RC800 despite its surface area suffering huge drop. This phenomenon could be caused by the location of the nickel that served as active sites was easily reached by the feed, lowering the mass transfer resistance that exist prior to diffusion of feed into catalyst [2].

Table 3 shows the catalyst selectivity towards liquid products based on GC-MS analysis. Although Ni/RC800 has the highest liquid yield, its product content was mainly organic, and it is the highest compared to the other catalysts. It seems like the impregnation of Ni

Table 2. The distribution of hydrocracking product

Catalyst	Conversion (wt%)			Residue (wt%)	Total Conversion (wt%)
	Liquid	Gas	Coke		
C800	60.13	38.29	0.13	1.45	98.55
RC800	52.56	44.57	1.51	1.36	98.64
Ni/C800	52.22	45.39	0.49	1.90	98.10
Ni/RC800	66.01	32.80	0.90	0.29	99.71

metal in RC800 was favoring the formation of organic fraction. This phenomenon could happen because of poor porosity properties of Ni/RC800 despite having additional acid active sites.

Although RC800 has better porosity properties and milder acidity compared to Ni/RC800, it produces larger gas fraction, which indicates there is overcracking phenomena. The overcracking phenomena could occurred when the reaction frequency was too high, usually caused by poor porosity properties or poor metal dispersion [2]. The overcracking was also happened to Ni/C800 catalyst, as the impregnated metal was not distributed evenly, proofed by the major downfall of the porosity properties. The feed does not have to diffused inside the pores and would easily reacts with the metal that is blocking the pores. Because of lack of diffusion control, the reaction frequency is too high and leads to over cracking phenomenon.

4. Conclusions

In this research, we found that H_2O_2 could act as activator that creates pores and gives oxygenated functional groups. The additional nickel in Ni/RC800 was beneficial and found to be the best catalyst where it gives liquid product conversion of 66.01 wt%. Its selectivity towards gasoline fraction, diesel fraction, alcohol, and organic was 8.06, 1.17, 2.61, and 54.13%, respectively.

Acknowledgements

This work was supported by Direktorat Sumber Daya, Direktorat Jenderal Pendidikan Tinggi, Riset dan Teknologi, Kementerian Pendidikan, Kebudayaan, Riset, dan Teknologi (Contract No. 7277/UN1/DITLIT/DITLIT/PT/2021).

References

[1] Das, M., Sarkar, M., Datta, A., Santra, A.K. (2018). An experimental study on the combustion, performance and emission characteristics of a diesel engine fueled with diesel-castor oil biodiesel blends. *Renewable Energy*, 119, 174-184. DOI: 10.1016/j.renene.2017.12.014

[2] Trisunaryanti, W., Sumbogo, S.D., Mukti, R.R., Kartika, I.A. (2021). Performance of low-content Pd and high-content Co, Ni supported on hierarchical activated carbon for the hydrotreatment of Calophyllum inophyllum oil (CIO). *Reaction Kinetics, Mechanisms and Catalysis*, 134(1), 259-272. DOI: 10.1007/s11144-021-02060-2

[3] Trisunaryanti, W., Larasati, S., Bahri, S., lailun Ni'mah, Y., Efiyanti, L., Amri, K., Nuryanto, R., Sumbogo, S.D. (2020). Performance comparison of Ni-Fe loaded on NH2-functionalized mesoporous silica and beach sand in the hydrotreatment of waste palm cooking oil. *Journal of Environmental Chemical Engineering*, 8(6), 104477. DOI: 10.1016/j.jece.2020.104477

[4] Trisunaryanti, W., Mukti, R.R., Kartika, I.A., Firda, P.B.D., Sumbogo, S.D., Prasetyoko, D., Bahruji, H. (2020). Highly selective hierarchical ZSM-5 from kaolin for catalytic cracking of Calophyllum inophyllum oil to biofuel. *Journal of the Energy Institute*, 93(6), 2238-2246. DOI: 10.1016/j.joei.2020.06.006

[5] Trovati, G., Suman, M.V.N., Sanches, E.A., Campelo, P.H., Neto, R.B., Neto, S.C., Trovati, L.R. (2019). Production and characterization of polyurethane castor oil (Ricinus communis) foam for nautical fender. *Polymer Testing*, 73, 87-93. DOI: 10.1016/j.polymertesting.2018.11.010

[6] Ganesan, R., Subramaniam, S., Paramasivam, R., Sabir, J.S., Josephin, J.F., Brindhadevi, K., Pugazhendhi, A. (2021). A study on biofuel produced by catalytic cracking of mustard and castor oil using porous Hß and AlMCM-41 catalysts. *Science of The Total Environment*, 757, 143781. DOI: 10.1016/j.scitotenv.2020.143781

Table 3. The catalyst selectivity towards fraction of liquid product

Catalyst	Fraction of liquid product (%)				Total liquid product (%)
	C_5-C_{12}	C_{13}-C_{18}	Alcohol	Organic	
C800	8.17	0.35	4.81	45.92	60.13
RC800	4.32	0.54	0.54	46.77	52.56
Ni/C800	6.32	1.22	3.07	41.14	52.22
Ni/RC800	8.06	1.17	2.61	54.13	66.01

[7] Keera, S.T., El Sabagh, S.M., Taman, A.R. (2018). Castor oil biodiesel production and optimization. *Egyptian Journal of Petroleum*, 27(4), 979-984. DOI: 10.1016/j.ejpe.2018.02.007

[8] Wijaya, K., Ariyanti, A.D., Tahir, I., Syoufian, A., Rachmat, A. (2018). Synthesis of Cr/Al_2O_3-Bentonite Nanocomposite as the hydrocracking catalyst of Castor oil. In *Nano Hybrids and Composites* (Vol. 19, pp. 46-54). Trans Tech Publications Ltd. DOI: 10.4028/www.scientific.net/NHC.19.46

[9] Wijaya, K., Syoufian, A., Fitroturokhmah, A., Trisunaryanti, W., Adi Saputra, D. (2019). Chrom/Nanocomposite ZrO_2-Pillared Bentonite Catalyst for Castor Oil (Ricinus communis) Hydrocracking. In *Nano Hybrids and Composites* (Vol. 27, pp. 31-37). Trans Tech Publications Ltd. DOI: 10.4028/www.scientific.net/NHC.27.31

[10] Saab, R., Polychronopoulou, K., Zheng, L., Kumar, S., Schiffer, A. (2020). Synthesis and performance evaluation of hydrocracking catalysts: A review. *Journal of Industrial and Engineering Chemistry*, 89, 83-103. DOI: 10.1016/j.jiec.2020.06.022

[11] Serrano, D.P., Melero, J.A., Morales, G., Iglesias, J., Pizarro, P. (2018). Progress in the design of zeolite catalysts for biomass conversion into biofuels and bio-based chemicals. *Catalysis Reviews*, 60(1), 1-70. DOI: 10.1080/01614940.2017.1389109

[12] Saab, R., Polychronopoulou, K., Zheng, L., Kumar, S., Schiffer, A. (2020). Synthesis and performance evaluation of hydrocracking catalysts: A review. *Journal of Industrial and Engineering Chemistry*, 89, 83-103. DOI: 10.1016/j.jiec.2020.06.022

[13] Li, T., Zhang, L., Tao, Z., Hu, C., Zhao, C., Yi, F., ... & Li, Y. (2020). Synthesis and characterization of amorphous silica-alumina with enhanced acidity and its application in hydroisomerization/cracking. *Fuel*, *279*, 118487. DOI: 10.1016/j.fuel.2020.118487

[14] Huang, P., Min, L.I.U., Chang, Q.L. (2020). MoO_3/Al-SBA-15 modified catalyst and its application in coal tar hydrocracking. *Journal of Fuel Chemistry and Technology*, 48(9), 1079-1086. DOI: 10.1016/S1872-5813(20)30072-4

[15] Danilova, I.G., Dik, P.P., Sorokina, T.P., Gabrienko, A.A., Kazakov, M.O., Paukshtis, E.A., Doronin, V.P., Klomov, O.V., Noskov, A.S. (2021). Effect of rare earths on acidity of high-silica ultrastable REY zeolites and catalytic performance of NiMo/REY+ Al_2O_3 catalysts in vacuum gas oil hydrocracking. *Microporous and Mesoporous Materials*, 329, 111547. DOI: 10.1016/j.micromeso.2021.111547

[16] Santi, D., Trisunaryanti, W., Falah, I.I. (2020). Hydrocracking of pyrolyzed α-cellulose to hydrocarbon over MxOy/Mesoporous carbon catalyst (M= Co and Mo): Synthesis and characterization of carbon-based catalyst support from saw waste of Merbau wood. *Journal of Environmental Chemical Engineering*, 8(3), 103735. DOI: 10.1016/j.jece.2020.103735

[17] Heidarinejad, Z., Dehghani, M.H., Heidari, M., Javedan, G., Ali, I., Sillanpää, M. (2020). Methods for preparation and activation of activated carbon: a review. *Environmental Chemistry Letters*, 18(2), 393-415. DOI: 10.1007/s10311-019-00955-0

[18] Xue, Y., Du, C., Wu, Z., Zhang, L. (2018). Relationship of cellulose and lignin contents in biomass to the structure and RB-19 adsorption behavior of activated carbon. *New Journal of Chemistry*, 42(20), 16493-16502. DOI: 10.1039/C8NJ03007C

[19] Rodríguez Correa, C., Stollovsky, M., Hehr, T., Rauscher, Y., Rolli, B., Kruse, A. (2017). Influence of the carbonization process on activated carbon properties from lignin and lignin-rich biomasses. *ACS Sustainable Chemistry & Engineering*, 5(9), 8222-8233. DOI: 10.1021/acssuschemeng.7b01895

[20] Cheng, J., Zhang, Z., Zhang, X., Liu, J., Zhou, J., Cen, K. (2019). Hydrodeoxygenation and hydrocracking of microalgae biodiesel to produce jet biofuel over $H_3PW_{12}O_{40}$-Ni/hierarchical mesoporous zeolite Y catalyst. *Fuel*, 245, 384-391. DOI: 10.1016/j.fuel.2019.02.062

[21] Gao, Y., Yue, Q., Gao, B., Li, A. (2020). Insight into activated carbon from different kinds of chemical activating agents: A review. *Science of the Total Environment*, 141094. DOI: 10.1016/j.scitotenv.2020.141094

[22] Liew, R.K., Chong, M.Y., Osazuwa, O.U., Nam, W.L., Phang, X.Y., Su, M.H., Chen, C.K., Chong, C.T., Lam, S.S. (2018). Production of activated carbon as catalyst support by microwave pyrolysis of palm kernel shell: a comparative study of chemical versus physical activation. *Research on Chemical Intermediates*, 44(6), 3849-3865. DOI: 10.1007/s11164-018-3388-y

[23] Prakash, M.O., Raghavendra, G., Ojha, S., Panchal, M. (2021). Characterization of porous activated carbon prepared from arhar stalks by single step chemical activation method. *Materials Today: Proceedings*, 39, 1476-1481. DOI: 10.1016/j.matpr.2020.05.370

[24] Luo, Y., Street, J., Steele, P., Entsminger, E., Guda, V. (2016). Activated carbon derived from pyrolyzed pinewood char using elevated temperature, KOH, H_3PO_4, and H_2O_2. *BioResources*, 11(4), 10433-10447.

[25] Danish, M., Ahmad, T. (2018). A review on utilization of wood biomass as a sustainable precursor for activated carbon production and application. *Renewable and Sustainable Energy Reviews*, 87, 1-21. DOI: 10.1016/j.rser.2018.02.003

[26] Sriningsih, W., Saerodji, M.G., Trisunaryanti, W., Armunanto, R., Falah, I.I. (2014). Fuel production from LDPE plastic waste over natural zeolite supported Ni, Ni-Mo, Co and Co-Mo metals. *Procedia Environmental Sciences*, 20, 215-224. DOI: 10.1016/j.proenv.2014.03.028

[27] Trisunaryanti, W., Larasati, S., Triyono, T., Paramesti, C., Santoso, N.R. (2020). Selective production of green hydrocarbons from the hydrotreatment of waste coconut oil over Ni- and NiMo-supported on amine-functionalized mesoporous silica. *Bulletin of Chemical Reaction Engineering & Catalysis*, 15(2), 415-431. DOI: 10.9767/bcrec.15.2.7136.415-431